Pulse Jitter Analysis

Pranav Kalsi*
Indian Institute of Science, Bangalore

April 28, 2024

This is an initial report of the work done by me so far for NIUS Astronomy project under guidance of Prof. Bhal Chandra Joshi.

1 Introduction

Astronomy is the science of observing and understanding our ultimate Universe and coming up with theories which match the observations. Our vast cosmos is a giant laboratory where experiments are conducted at unimaginable scales that can never be replicated on our pale blue dot. This gives us an opportunity to extrapolate our understanding of local physical world and test our theories in extreme conditions. Few years back , electromagnetic radiation was the primary language that we used to understand our cosmos. But after the discovery/detection of gravitational waves we learned a new way to explore and understand our universe. Pulsar timing experiments will help us learn more about low frequency gravitational waves emerging from supermassive black holes during galaxy mergers.
This project will help me learn the techniques used in Pulsar timing and give me an opportunity to appreciate and contribute to the understanding of our universe.

2 Radio Astronomy(1)

Radio astronomy is the study of natural radio emission from the celestial sources. The range of radio frequencies or wavelengths are loosely defined by atmospheric opacity and by quantum noise in coherent amplifiers. Together they place the boundary between radio and far-infrared astronomy frequency ν=1THz (1THz=10^{12}Hz) or wavelength λ=0.3mm.
The Earth's ionosphere sets a low frequency limit to ground based radio astronomy by reflecting extraterrestrial radio waves with frequency less than 10MHz(λ ∼30m) and the ionized interstellar medium of our own galaxy absorbs extra-glactic radio signals below ν ∼2MHz.(See figure1)

Since only optical and radio observations can be made from the ground , radio astronomers had the first opportunity to explore a "parallel universe" containing new objects such as radio galaxies, quasars and pulsars, plus very cold sources such as interstellar molecular clouds and the cosmic microwave background radiation from the big bang itself. The first confirmed discovery of extra-solar planets was made in 1992 by radio astronomers when a system of terrestrial-mass planet was found to be present around a pulsar(2).

2.1 Radio Telescopes

A radio telescope is a reciever which detects the oscillating voltage difference across its length because of propagating electromagnetic waves (radio waves). The natural radio signals are very weak and must be amplified. The use of amplifiers for the first stage of a receiver defines the boundary between radio and mm and sub-mm wave astronomy. At wavelengths longer than a few mm (below 100 GHz) low-noise transistor amplifiers (LNAs) are used; however, the laws of quantum mechanics require any amplifier to add noise to the signal, and at the shorter mm and sub-mm wavelengths transistor amplifiers generate too much self-noise. The extraneous noise signals also corrupt the observations and, almost always, the cosmic radio signal is far weaker than the extraneous noise. So how do we then detect a source whose signal level is very less than the extraneous noise level. The answer is to increase the amount of time of observation and take an average. Radio astronomers characterise and quantify signal (noise level) in the

*email: pranavkalsi@iisc.ac.in

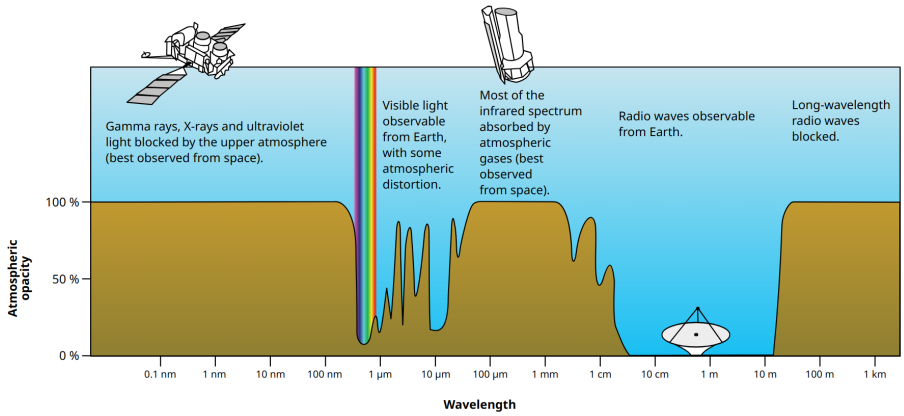

Figure 1: The figure shows opacity of earth's atmosphere at different wavelengths. The inosphere reflects of the wavelegths longer than 30 m, as a consequence we cannot observe at those frequencies from ground based observatories. [source]

units of temperature. Temperature of a source is defined as the temperature of a resistor when it heats up when you put power through it.

2.2 Antenna temperature[1]

Every body at a physical temperature higher than 0K emits electromagnetic radiation. Brightness(intensity) of the body as perceived by a receiver can be characterized by emmisivity of the body and its physical temperature. Also response of an antenna is not uniform to all the directions , which is characterized by a gain of the antenna. So we define antenna temperature (or antenna noise) as the brightness temperature of radio signal taking into account the gain factor. The following are the sources of antenna temperature:

1. radiation from the source or region under study, T_s
2. radiation from the cosmic microwave background, T_{cmb}
3. radiation from the Milky Way galaxy, T_{gal}
4. radiation from the atmosphere, T_{atm}
5. radiation picked up in the sidelobes of the beam, in most cases principally thermal noise from the ground, T_{sl}
6. thermal noise associated with losses in the antenna itself, in the transmission line, or in any passive components in the signal path before the low-noise amplifier, T_{loss}

The antenna temperature is the following sum:

$$T_A = T_s + T_{cmb} + T_{gal} + T_{atm} + T_{sl} + T_{loss} \tag{1}$$

The noise temperature for different sources is a function of frequency. We define T_{sys} as the temperature because of all other sources including the noise introduced by amplifiers.

$$T_{sys} = T_{cmb} + T_{gal} + T_{atm} + T_{sl} + T_{loss} + T_{LNA} \tag{2}$$

We see that it is the sum of independent components, one of which is known to very high accuracy (T_{cmb}), two of which may be measured to high (< 1 K) accuracy (T_{loss} and T_{LNA}) in the laboratory, and the others of which (T_{gal} , T_{atm} , and T_{sl}) can be assessed with reasonable accuracy (1–2 K at short wavelengths), depending on the dimensions of the telescope beam and the relative contribution of the side-lobes.

[1] refer section 5.3 Bernard F. Burke to learn more about antenna temperature

2.3 Radiometer equation

The radiometer equation is given by

$$\Delta T_{rms} = \frac{T_{sys}}{\sqrt{\Delta\nu\mathcal{T}}} \tag{3}$$

where $\Delta\nu$ is the bandwidth, $\mathcal{T}$ is the integration time. The signal-to-noise ratio (S/N) of an observation is given by:

$$S/N = \frac{T_{src}}{\Delta T_{rms}} = \frac{T_{src}}{T_{sys}}\sqrt{\Delta\nu\mathcal{T}} \tag{4}$$

So for detecting a very faint source, we need to make sure that $\mathcal{T}$ is long enough to have large S/N. Technique like interferrometry[2] offers us another way to increase S/N for same $\mathcal{T}$.

3 GMRT

Giant Meterwave Radio Telescope is an interferrometric array of 30 dishes of 45m diameter each, with a baseline of up to 25 Km. GMRT has 4 bands at which it operates [3]:

1. Band 2: 130-260 MHz
2. Band 3: 250-500 MHz
3. Band 4: 550-900 MHz
4. Band 5: 1000-1500 MHz

The electromagnetic waves (e.g. radio signals) coming for any source are measured as continuously varying voltage signals which can be broken down into sinusoidal components with different frequency, amplitude and phase.The incident electric field can have any polarization, so GMRT's feed consists of two perpendicular detectors which measure the voltage in both polarization states. GMRT or any radio telescope stores the amplitude of the voltage signal discretely by recording the voltage periodically after a finite amount of time called the sampling rate. This sampling rate has to be greater than twice the maximum frequency present in our signal (Nyquist–Shannon sampling theorem). Then the sampled data is divided into number of frequency channels by taking a Fourier transform . Thus the raw data consists of voltage amplitudes over different frequency channels and two orthogonal polarization states as a function of discrete time. So the data can be stored as discrete time series with square of voltage amplitudes (since it represents intensity) represented by an integer over different frequency channels and two polarization states. It can be represented by a 3D array , whose dimensions are frequency , polarization and time.
One can also estimate the size of this dataset

$$= N_{pol} \times \frac{t_{\text{Observation}}}{t_{\text{sampling}}} \times N_{\text{freq chan}} \times N_{\text{bits}}(\text{integer representing aplitude})$$

GMRT stores raw data as amplitude represented by a 16 bit number, let us estimate size of a typical 40 minute observation, at band 3 (max frequency = 500MHz , N_{freq}= 4096) , it turns out that size $\geq$36Gb .Such large data volumes are computationally very expensive and not portable, so one has to reduce the data volume before analysis.

3.1 Data reduction with PINTA(3)

Pipeline for the Indian pulsar Timing Array is the data reduction pipeline used for converting raw data(bits) into a user-friendly FITS(Flexible Image Transport System) format by partially folding the time series into n subints according to input parameters i.e converts raw data into a 4D array of 16 bit integers, whose extra extra dimension are partially folded profiles called subints. As an example we reduced the data of PSRJ1645-0317 using pinta. Here is a brief list of steps followed:

1. Create three directories named
   (a) `input_dir` : containing the .raw (raw data file) and .raw.hdr (header file or timestamp)

[2] refer chapter 9 Bernard F. Burke for further reading
[3] for more information refer GMRT official website

(b) `working_dir`: containing the pipeline.in file.

(c) `par_dir`: containing the .par file which can be generated as

```
psrcat -e Jmmmm+dddd > Jmmmm+nnnn.par

psrcat:  pulsar catalog
Jmmmm+dddd is the Jname of the pulsar
```

2. Running the following command

```
pintav6 --no-gptool --pardir par_dir input_dir working_dir
```

The details can be found here.

4 Pulsars

Pulsars were first discovered when Jocelyn Bell in 1967 found a periodic signal on chart recordings.[4] Existance of pulsars was first suggeted by Baade and Zwicky. They claimed that the final stage of evolution of a massive star would be a catastrophic collapse of its core, leading to a supernova explosion and leaving a small and very condensed remnant, a neutron star(4). Figure 2 shows the structure of a typical model neutron star with mass $1.4M_{\odot}$.

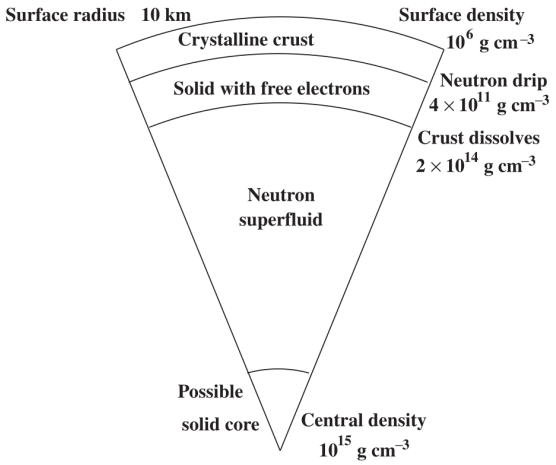

Figure 2: A section through a typical model neutron star [taken from Bernard F. Burke(5)].

Pulsars have very large surface magnetic fields, typically between 10^8 and 10^{14} gauss (10^{4-10} T).The strong magnetic field, combined with the rapid rotation, generates very strong electric fields outside the neutron star. These fields pull charged particles from the surface,forming a dense and highly conducting magnetosphere(6). The charged particles in this magnetic field gyrate at relativistic speed and emit highly beamed radiation. This beamed radiation is what detected by us as periodic pulses , since the rotation rate of pulsars is highly stable because of large angular momentum.

4.1 Rotation Slowdown

All pulsars slowdown overtime because they loose their kinetic energy either directly by magnetic dipole radiation or by an outflow of energetic particles accelerated by electromagnetic induction.

[4]Read this for the full discovery story in her own words.

4.2 Nulling, Moding, and Timing noise

In many pulsars the variability from pulse to pulse extends to a complete gap in emission lasting for a number of pulses. This pulse nulling may extend for long periods: there are pulsars which disappear for many hours or even for many days. In pulsars with several components there may be sudden changes in the observed integrated profile, switching between different patterns of mean excitation; this behaviour is known as moding. These changes in pulse profile are instantaneous, occurring at intervals of days, months, or years (7); they are accompanied by small switches in slowdown rate. In the analysis of pulse arrival times, intended to derive a rotation rate and its derivative, there is usually a residual component that is generally referred to as timing noise. It seems likely that this is a manifestation of the same instability as moding, but at a low level and often on a short timescale.

4.3 Propagation of pulses through intervening media

The intervening media affects the electromagnetic radiation emitted by pulsars. The magnetic fields result in Faraday rotation[5].The electron density may cause dispersion, as a result a broadband pulse moves through a plasma more slowly at lower frequencies than at higher frequencies. If the distance to the source is d, the dispersion delay t at frequency ν in astronomically convenient units is

$$(\frac{t}{sec}) \approx 4.149 \times 10^3 (\frac{DM}{pccm^{-3}})(\frac{\nu}{MHz})^{-2} \tag{5}$$

$$\text{where, DM} = \int_0^d n_e dl \tag{6}$$

is called the dispersion measure and represents the integrated column density of electrons between the observer and the pulsar. Dispersion measures can be used to provide distance estimates to pulsars. Crude distances can be calculated for pulsars near the Galactic plane by assuming that n_e ~0.03 cm^3.
The ionized ISM affects pulsar signals in several other ways besides dispersion. Inhomogeneities in the turbulent ISM result in both diffractive and refractive scintillation, or time- and frequency-dependent flux-density variations of the pulsar signal much like the "twinkling" of starlight by Earth's turbulent atmosphere. Diffractive scintillations occur over typical timescales of minutes to hours and radio bandwidths of kHz to hundreds of MHz, and they can cause more than order-of- magnitude flux-density fluctuations. Refractive scintillations tend to be less than a factor of ~2 in amplitude and occur on timescales of weeks.

5 Pulsar timing

Pulsar timing is the regular monitoring of the rotation of the neutron star by tracking the arrival times of the radio pulses. Pulsar timing accounts for every single rotation of the neutron star over long periods (years to decades) of time. This very precise tracking of rotation phase allows us to probe the interior physics of neutron stars, make extremely accurate astrometric measurements, uniquely test gravitational theories in the strong-field regime, and directly detect gravitational waves from supermassive black hole binaries. Pulsar timing observations have produced some of the most exciting results in pulsar astronomy and indeed in all of astronomy. For instance, such results have included the first detection of extra-solar planets(2), stringent tests of the general theory of relativity (8), revealed dispersion measure variations due to the interstellar medium, pulsar proper motions (9) and irregularities in the spin-down of pulsars. Pulsar timing is now being used to verify terrestrial time standards and the Solar System ephemeris and in searches for gravitational radiation(10).

5.1 PSRCHIVE(11)

PSRCHIVE is an Open Source C++ development library for the analysis of pulsar astronomical data. It implements an extensive range of algorithms for use in pulsar timing, scintillation studies, polarimetric calibration, single-pulse work, RFI mitigation, etc. These tools are utilized by a powerful suite of user-end programs that come with the library.

For pulsar timing, average (folded) the data from many pulses which yields an average pulse profile. Although the shapes of individual pulses vary considerably because pulsar emission is intrinsically a noise

[5]read section 14.10 Bernard F. Burke for more information

process also there are other sources noise which make up the signal read by the detector,but the shape of the average profile (template) is quite stable. Average profile of a pulsar is considered as its fingerprint signature.
A template profile is prepared by averaging out all the subintegrations using pam command in PSRCHIVE while preserving the frequency subbands. Time collapsed data is then dedispersed to obtain noise free template using wavelet filter implemented in psrsmooth command.
For timing, the subints are cross-correlated with the template so that its phase offset can be determined. When multiplied by the instantaneous pulse period, that phase yields a time offset that can be added to a high-precision reference point on the profile (for example, the left edge of the profile based on the recorded time of the first sample of the observation) to create the time of arrival (TOA). This is done by using pat command in PSRCHIVE
The precision with which a TOA can be determined is approximately equal to the duration of a sharp pulse feature (e.g., the leading edge) divided by the signal-to- noise ratio of the average profile. It is usually expressed in terms of the width W_f of the pulse features in units of the pulse period P , and the signal-to-noise ratio (S/N) such that:

$$\sigma_{\mathrm{TOA}} \propto W_f \frac{P}{(S/N)} \tag{7}$$

Strong, fast pulsars with narrow pulse profiles provide the most accurate arrival times.

A In this section we will analyse PSRJ1645-0317 [6] data. The goal of the analysis is to understand effect of number of averaged subints (folded profiles) on signal-to-noise ratio as $\sigma_{\mathrm{TOA}} \propto \frac{1}{S/N}$ and theoretically $\frac{1}{S/N} \propto \sqrt{N}$, where N is the number of integrated subints.
We follow the following steps:

1. Obtain average pulse profiles by taking average of 4, 16 , 64 ,256 and 1024 subints.5
2. Compute the signal-to-noise ratio for different profile and plot them as a function of N.6

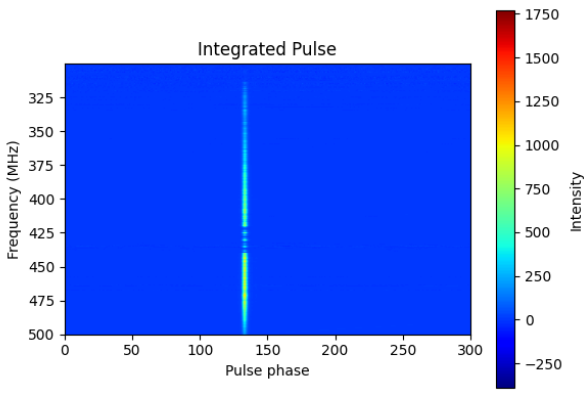

Figure 3: The integrated pulse profile of 2404 subints.Each subint was formed after partially folding 3 pulses of original data during data reduction process with pinta.

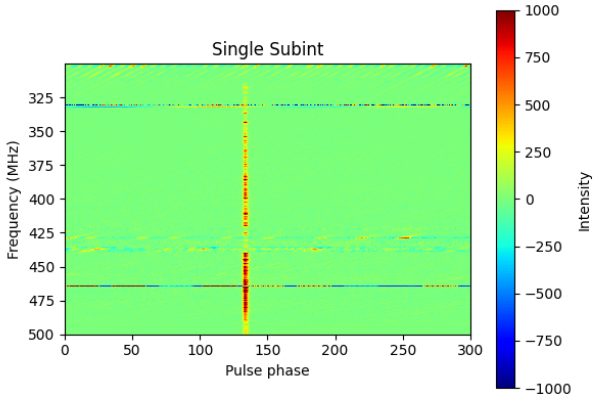

Figure 4: This is the plot of a single subint which consist of 3 folded pulses from original raw data. We see streaks at some frequencies because of rfi's as we did not remove rfi's during data reduction process with pinta

[6] Nomenclature

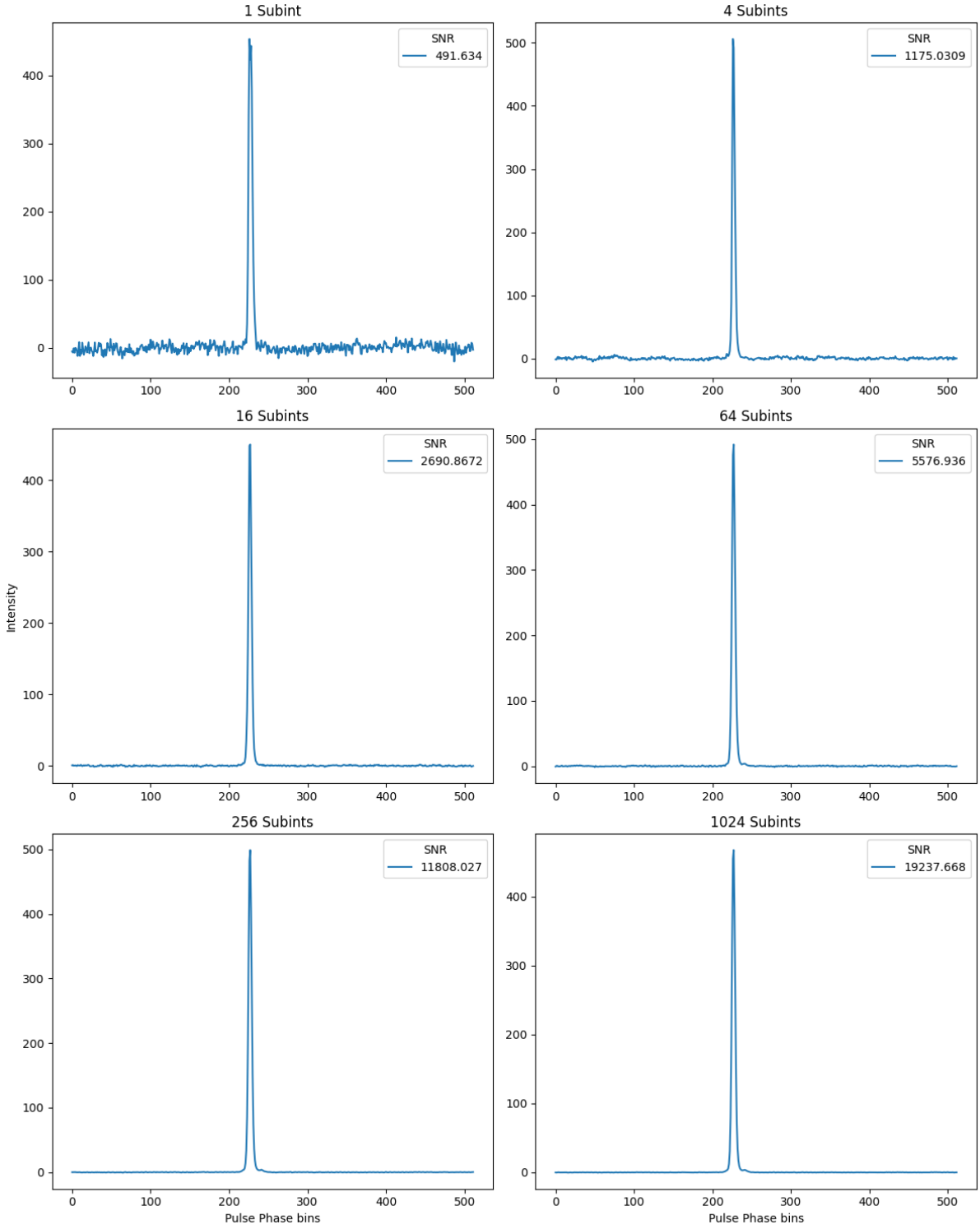

Figure 5: We clearly see a difference in the noise level as number of subints int the averaged profile increase.

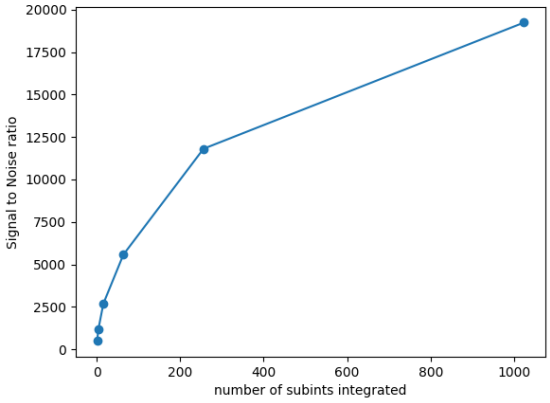

Figure 6: The plot is in aggrement with $snr \propto \sqrt{N}$

5.2 Tempo2(12)

The TOAs we obtained by PSRCHIVE are in reference to observatory's time. These TOAs need adjustment so that they represent arrival times in an inertial reference frame . This is accomplished by transforming each measured arrival time to an arrival time in the reference frame of the pulsar by first calculating arrival times at the Solar System barycentre (SSB) and then, if necessary, including additional terms required to model the pulsar's orbital motion. Tempo2 helps us in coming up with a timing model, that captures the pulsar's spin-down behaviour by fitting the residuals of measured TOAs with the ones predicted. If significant systematic deviations are seen when calculating the differences between the actual arrival times and the best-fit model arrival times (known as timing residuals) then it is clear that the model is not fully describing the true pulsar parameters; a positive residual corresponds to the pulse arriving later than predicted. Such discrepancies can be due to many effects including unmodelled binary companions or binary parameters, irregularities in the spin-down of the pulsar, or poor estimation of the astrometric or rotational parameters. For instance, an incorrect estimate of the pulsar's position or its proper motion leads to a poor determination of the barycentric arrival times, which will produce a sinusoidal feature in the timing residuals. This timing technique therefore allows pulsar parameters to be measured extremely precisely; the precision improves with longer data sets and more accurate TOA measurements.

In this section we will come up with a timing model of PSRJ1645-0317 using the TOA's generated by PSRCHIVEA. The goal of this analysis is to observe the residuals as we make model the measure TOAs for different subintegrations that we generated from PSRCHIVE.We analysed the data of PSRJ1645-0317 with PSRchive and the following section documents the process we followed.

1. We generate a template profile with PSRCHIVE's `tscrunch_to_nsub(1)` Python function which crunches all the subints into 1 keeping the existing 64 frequency bands as it is.

2. Then we smoothen the integrated profile with `psrsmooth` command.

   ```
   psrsmooth -W <Integrated Profile>
   ```

   -W stands for wavelet transform (uses sinc function by default). It takes the wavelet transform of the integrated profile and generating the smoothed template by rejected high frequency modes which are because of noise and then takes back inverse wavelet transform, thus generating a smooth template.

3. Then we generate TOAs with `pat` command

   ```
   pat -s <Template> -f 'tempo2' -F <partialy_folded_subints> > TOAs.tim
   ```

4. Then we run tumpo2 by giving ephemeris file generated by psrcat and .tim file generated from previous step.

Here is the prefit and postfit residual plot in tempo2 after averaging 16 and subints.

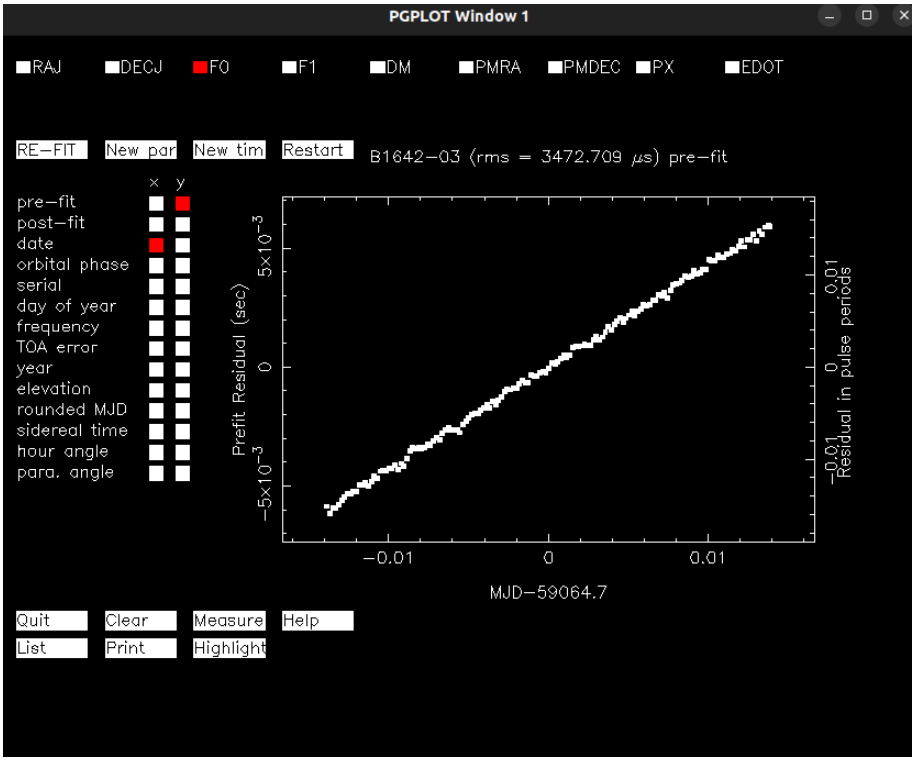

Figure 7: The prefit rms= 3472.709μs

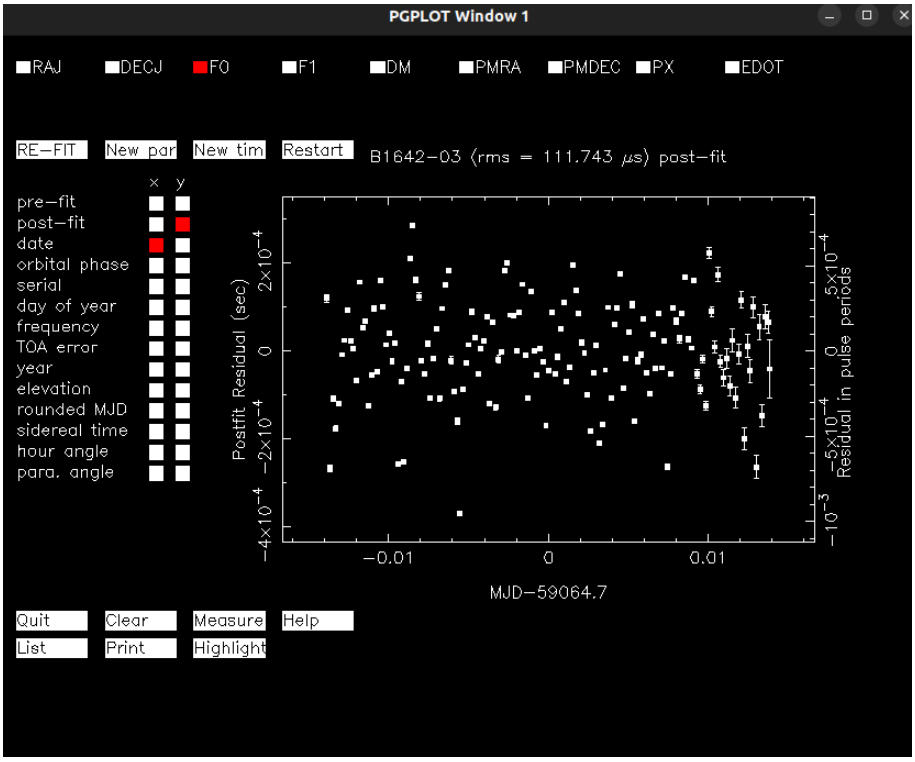

Figure 8: Postfit rms= 111.743μs, ΔF_0=-1.283910$^{-5}s^{-1}$

Table 1: rms of residuals post fitting F_o(pre-fit value =2.57938244186282 s^{-1})

Number of Subints combined	Pre-fit residual rms(μs)	Post-fit residual rms(μs)	Difference ΔF_0 $10^{-5}(s^{-1})$
4	3462.551	228.603	-1.2843
16	3472.709	111.743	-1.2839
64	3492.789	69.387	-1.2846
256	3600.089	21.051	-1.2838
1024	3504.505	0.556	-1.2838

6 Results

1. We observed that signal-to-noise ratio grows as $\sqrt{\mathrm{N}}$, where N is the number of subints. 6
   So, we expect $\sigma_{\mathrm{TOA}} \propto \frac{1}{\sqrt{\mathrm{N}}}$.

2. We also observed that rms of timing residuals after fitting in tempo2 also decreases as $1/\sqrt{N}$.1

The above result is a consequence of the law of large numbers. The pulsar signal received can be thought as a random variable with a mean value as average pulse profile and jitter as noise function. In addition to jitter noise , pulses are affected by radiometer noise 2.3 which has a finite mean value and a standard deviation. As we increase the number of subintegrations N, the standard deviation decreases as $1/\sqrt{\mathrm{N}}$. Hence the same is observed in the TOAs.

References

Scott M. Ranson James J. Condon. *Essential Radio Astronomy*. Princeton University Press, 2016.

D.A.Frail 1992 A. Wolszczan. A planetary system around the millisecond pulsar psr1257 + 12. *Nature*, 355:145–147, 1992.

Abhimanyu Susobhanan, Yogesh Maan, Bhal Chandra Joshi, T. Prabu, Shantanu Desai, K. Nobleson, Sai Chaitanya Susarla, Raghav Girgaonkar, Lankeswar Dey, Neelam Dhanda Batra, and et al. pinta: The ugmrt data processing pipeline for the indian pulsar timing array. *Publications of the Astronomical Society of Australia*, 38:e017, 2021.

D. E. Osterbrock. Who Really Coined the Word Supernova? Who First Predicted Neutron Stars? In *American Astronomical Society Meeting Abstracts*, volume 199 of *American Astronomical Society Meeting Abstracts*, page 15.01, December 2001.

Bernard F. Burke, Francis Graham-Smith, and Peter N. Wilkinson. *An Introduction to Radio Astronomy*. Cambridge University Press, 4 edition, 2019.

Peter Goldreich and William H. Julian. Pulsar Electrodynamics. , 157:869, August 1969.

Andrew Lyne, George Hobbs, Michael Kramer, Ingrid Stairs, and Ben Stappers. Switched magnetospheric regulation of pulsar spin-down. *Science*, 329(5990):408–412, 2010.

Ingrid H. Stairs. Testing general relativity with pulsar timing. *Living Reviews in Relativity*, 6(1), September 2003.

M. Kramer, A. G. Lyne, G. Hobbs, O. Lhmer, P. Carr, C. Jordan, and A. Wolszczan. The proper motion, age, and initial spin period of psr j0538+2817 in s147. *The Astrophysical Journal*, 593(1):L31–L34, July 2003.

Fredrick A. Jenet, George B. Hobbs, K. J. Lee, and Richard N. Manchester. Detecting the stochastic gravitational wave background using pulsar timing. *The Astrophysical Journal*, 625(2):L123–L126, May 2005.

Willem van Straten, Paul Demorest, and Stefan Osłowski. Pulsar data analysis with psrchive, 2012.

R. N. Manchester G. B. Hobbs, R. T. Edwards. Tempo2, a new pulsar timing package. i: Overview, 2006.

A Appendix 1:Notebook

Here is the link to notebook file.